Single Phase VSI Behavior Improvement using Combined Feedback and Feedforward Controllers

MOHAMMAD A. OBEIDAT
Department of Electrical Power and Mechatronics Engineering, College of Engineering,
Tafila Technical University,
Tafila 66110, JORDAN

MUSTAFA ALZGHOUL
Jordan Customs, Engineering Department,
Amman, JORDAN

KHALED A. MAHAFZAH
Electrical Engineering Department, College of Engineering,
Al-Ahliyya Amman University,
Amman 19328, JORDAN

HESHAM AL SALEM
Department of Mechanical Engineering, College of Engineering,
Tafila Technical University,
Tafila, 66110, JORDAN

Abstract: - Nowadays, the demand for power electronics technology has increased due to the importance of its applications such as power inverters. The power inverter is required to modify the DC power from PV cells to AC power. One of the most common issues of on-grid PV systems is the high variations of the generated DC voltage. This will affect the stability of the generated AC voltage at the Point of Common Coupling (PCC) with the grid. This paper combines the Feed-Forward and Feedback (FFFB) controller in a novel way to reduce the variation of the PV cells DC voltage. This paper presents both mathematical and Simulink models of single-phase voltage source inverters VSI. Then, a case study of 15% disturbance of DC-generated voltage is considered. The static and dynamic behaviour of the single-phase H-bridge inverter is analysed under different loads. The new combination is used to reduce the effect of the disturbance on the performance of the system. Also, the proposed closed-loop controller (FFFB) can reduce the overshoot by 50% less than the feedback controller only. The settling time has been improved by 41%, 61% for RL and induction motor.

Key-Words: - Voltage Source Inverter, Feedback control, Feed-forward control, Combined Controller, Disturbance rejection.

Received: March 16, 2022. Revised: November 7, 2022. Accepted: December 8, 2022. Published: December 31, 2022.

1 Introduction

Power electronics transform electric power from one form to another with different features. Around 70% of electricity in the US is now running by power electronics, which will gradually increase to 100 percent, [1]. Smart Grids (SG) provides more adaptable, stable, and sustainable power systems. It integrates many types of power sources effectively, [2]. Solar energy is typically extracted from a Photovoltaic (PV) cell that converts solar irradiance into Direct Current (DC), where an inverter is required to modify the generated DC power from the PV cell to Alternating Current (AC) electricity, [3].

The inverter forms aback-bone of diving systems, integration of PVs with electrical grids. The inverter comprises a DC voltage source, DC link capacitor, two switching devices (half bridge invert-er), four switching devices (H-bridge inverter), or six switching devices (three-phase inverter). Additionally, it has freewheeling diodes to guarantee a bidirectional current flow, [4]. Load variations during the operation of the inverter is one crucial issue since it causes a voltage

fluctuation. This affects the power quality of the supplied power and increases the output current ripple, [5]. Hence, it reduces the inverter's efficiency, [6], [7].

Regarding voltage fluctuations, more attention has been paid in literature. In [8], the authors introduced the voltage fluctuation issue at the output of a single-phase inverter due to the voltage disturbances of the coupling capacitor. The researchers showed that the fluctuation of the DC link voltage directly affected the input current, thus, the maximum power tracking. The control strategy was compensating the voltage and the current of the capacitor bus using two Proportional Integral (PI) controllers. To verify their results, a 3-kW prototype was investigated to realize the ability of the control technique. In [9] the researchers proposed the double closed loop control based on ADRC to reduce the excessive voltage disturbances, and low harmonics of voltage source inverter. The adopted approach was compared to the conventional use of PID control method, and the results showed that the proposed method provided better performance compared to PID, and accordingly the authors recommended its use in grid connected application. In [10], the authors reviewed two strategies to regulate the output voltage of the grid connected inverters. Power curtailment and reactive power compensation were introduced to control the inverter voltage under high PV penetration.

Many of the voltage quality were reviewed such as voltage rise, voltage harmonics, DC injection, voltage dips and voltage unbalance. In [11], the authors replaced the use of filters by current control strategies to minimize the harmonics and to regulate the voltage of single-phase grid connected inverters. Current Hysteresis Control (CHC), Voltage Oriented Control (VOC) and Proportional Resonant based (PR-based) control were conducted and compared. The obtained results showed that VOC and PR-based provided the better performance in terms of volt-age regulation, dynamic response, and harmonics distortion minimization. In [12], the optimized feed-forward controller of DC-DC converter is used to achieve almost zero DC audio susceptibility. The proposed method was presented based on the non-optimal operation between the input-output voltages of the DC converters. In [13], the authors proposed a state feedback current controller depending on the Equivalent Input Disturbance (EID) to adjust the current of the grid tied inverter and to achieve the maxi-mum power point tracking. The results confirmed the excellence of the adopted approach. In [14], an adaptive feed-forward control strategy is applied to solve the jumping disturbance issue at the input voltage of the DC-DC boost converter. The adopted approach combined feedback and adaptive feed-forward control techniques. The obtained results showed the effective performance of the explored approach. In [15], the researchers proposed the feed-forward/feedback technique to tune the classical pole placement controller for the single Input Single Output (SISO) system. The control strategy was tested on both mathematical and physical models of the plant. The results recommended that the adopted approach achieved excellent responses with zero steady state error under the load variation. In [16], the author proposed the feed-forward/feedback control strategy depending on the Deep Q-learning Network (DQN) for liquid level regulation under various disturbances. The adopted approach was compared with the conventional PID feedback system. The obtained results showed the supremacy of the proposed strategy.

In [17], the authors introduced a dual control method to regulate the voltage of multi-micro grid inverters. The adopted approach utilized the feed-forward/feedback control structure to enhance the transient response, to reduce the steady state error and to optimize the performance of the controller. The feedback system was converted into an optimization problem with linear objective functions. The experimental results proved the effective performance of the proposed approach in terms of voltage regulation, harmonics rejection, and fault condition operation.

The importance of this paper relies on developing a new merged control method based on feedback and a feed-forward controller for input disturbance disposal of a single-phase voltage source inverter (VSI-H bridge). The mathematical model of the VSI-H-bridge has been built. Then, the DC disturbance mathematical model has been established in the case of static and dynamic loads. To show the effectiveness of the proposed new control method, its results are compared with the DC input voltage of the VSI-H bridge when using a conventional PID with feedback. The results and discussion show the superior of the new control method.

This paper is organized as follows: section 1 introduces the literature review. The mathematical model of single phase VSI is presented in section

2. Section 3 proposes the FFFB system of single phase VSI under different loads. The simulation results and discussion are presented in section 4. Finally, the paper is concluded in section 5.

2 VSI-H Bridge Inverter Mathematical Modelling

In this section, the VSI-H bridge inverter design will be illustrated along with control structures of feedback and feed-forward/feedback control systems. The inverter filter circuit will be explained as well.

2.1 VSI-H Bridge Implementation

The VSI-H bridge as shown in Figure 1 comprises two arms, each with two switching devices and antiparallel freewheeling diodes for discharging the inverse current. The inverse load current flows through these diodes in the case of dynamic load. These diodes offer an alternative direction for inductive current, which continues to flow even though the switch is turned off.

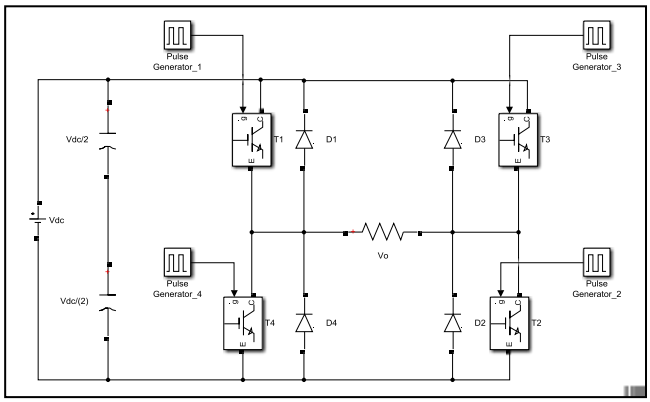

Fig. 1: VSI-H bridge inverter.

T_1, T_2, T_3, and T_4 are switching devices. The switches in each branch are switched alternately such that they are not in the same state (ON / OFF) at the same time. In operation, they are both turned off for a brief amount of time known as blanking time (dead time) to prevent cross-through of the operation. To obtain the output, the switches T_1 and T_2 or T_3 and T_4 must be operated simultaneously. Table 1 showed the switching state of the half-bridge inverter.

Table 1. Full bridge inverter switching states

T_1	T_2	T_3	T_4	V_o
ON	*ON*	*OFF*	*OFF*	$+V_{dc}$
OFF	*OFF*	*ON*	*ON*	$-V_{dc}$
ON	*OFF*	*ON*	*OFF*	**Zero**
OFF	*ON*	*OFF*	*ON*	**Zero**

The PWM VSIs are the most appropriate ones in the industry. It is used to retain the inverter's output voltage at the rated voltage independent of the output load. PWM is a technique that generates constant amplitude pulses by altering the pulse duration by controlling the duty cycle. Analog PWM control necessitates the generation of both fundamental and carrier signals, which are fed into the comparator and the final output is generated based on some logical output. The fundamental signal is the target signal source, which may be a sinusoidal or square wave, while the carrier signal is either a saw-tooth or triangular wave of a much higher frequency than the fundamental signal, [23], [24], [25], [26].

To reduce harmonics produced by the pulsating modulation waveform, a low pass LC filter is necessary at the VSI-H bridge output terminal. The cut-off frequency of an LC filter is selected so that the majority of the low order harmonics are omitted. To operate as an ideal voltage source with no additional voltage distortion under load variations or nonlinear loads, the inverter's output impedance must be held at zero. Therefore, the capacitance and the inductance of the selected filter should be maximized and minimized respectively, [18], [19], [20], [21], [22]. See Figure 2.

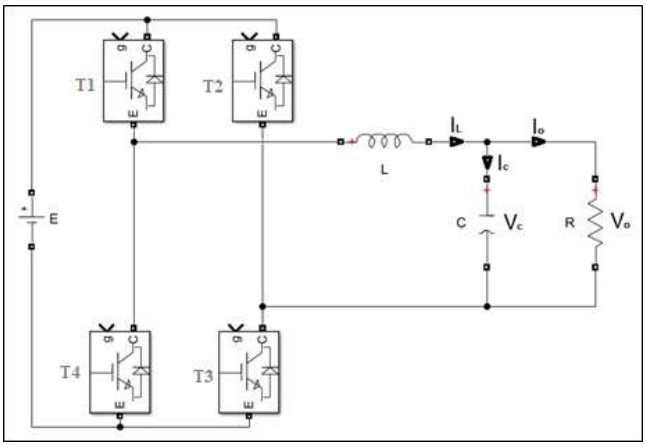

Fig. 2: VSI-H bridge with resistive load.

2.2 VSI-H Bridge State Space Implementation

The full bridge single phase inverter with resistive load will be modelled by deriving the operation states equations as follow the state space representation for state (1) will be:

$$-E + L\frac{di_L}{dt} + V_c = 0 \quad (1)$$

$$\frac{dV_c}{dt} = \frac{1}{C}(i_L - i_O) \quad (2)$$

$$\frac{di_L}{dt} = \frac{1}{L}(E - V_c) \quad (3)$$

$$\frac{dV_c}{dt} = \frac{1}{C}(i_L - \frac{V_c}{R}) \quad (4)$$

$$V_o = V_c$$

The state space representation for state (1) will be:

$$X^{\cdot} = A_1X + B_1E$$
$$Y = C_1X + D_1E \quad (5)$$

Where

$$X = [i_L \quad V_c \quad i_o]^T \quad (6)$$

$$A_1 = \begin{bmatrix} 0 & \frac{-1}{L} & 0 \\ \frac{1}{C} & 0 & \frac{-1}{C} \\ 0 & \frac{1}{L_f} & \frac{-R_f}{L_f} \end{bmatrix} \qquad B_1 = \begin{bmatrix} \frac{1}{L} \\ 0 \\ 0 \end{bmatrix} \quad (7)$$

$$C_1 = [0 \quad 1 \quad 0] \qquad D_1 = [0]$$

For State (2): at the negative half cycle, T_2 and T_4 are ON, applying KVL, then:

$$-E + L\frac{di_L}{dt} - V_c = 0 \quad (8)$$

$$\frac{dV_c}{dt} = \frac{1}{C}(i_L - i_O) \quad (9)$$

$$\frac{di_L}{dt} = \frac{-1}{L}(E + V_c) \quad (10)$$

$$\frac{dV_c}{dt} = \frac{1}{C}(i_L - \frac{V_c}{R}) \quad (11)$$

$$V_o = V_c \quad (12)$$

The state space representation for state (2) will be:

$$X^{\cdot} = A_2X + B_2E$$
$$Y = C_2X + D_2E \quad (13)$$

Where

$$X = [i_L \quad V_c]^T$$

$$A_2 = \begin{bmatrix} 0 & \frac{-1}{L} \\ \frac{1}{C} & \frac{-1}{RC} \end{bmatrix} \qquad B_2 = \begin{bmatrix} \frac{-1}{L} \\ 0 \end{bmatrix} \quad (14)$$

$$C_2 = [0 \quad 1] \qquad D_2 = [0]$$

State space averaging technique is used to combine both of the two operation states in one state space representation as follows:

$$X^{\cdot} = d.(A_1X + B_1E) + (1-d).(A_2X + B_2E)$$
$$Y = d.(C_2X + D_2E) + (1-d).(C_2X + D_2E)$$

$$X^{\cdot} = \begin{bmatrix} 0 & \frac{-d}{L} \\ \frac{d}{C} & \frac{-d}{RC} \end{bmatrix} X + \begin{bmatrix} \frac{d}{L} \\ 0 \end{bmatrix} E + \begin{bmatrix} 0 & \frac{-1}{L} + \frac{d}{L} \\ \frac{1-d}{C} & \frac{-1+d}{RC} \end{bmatrix} X + \begin{bmatrix} \frac{-1}{L} + \frac{d}{L} \\ 0 \end{bmatrix} E$$

$$Y = d.([0 \quad 1]X) + (1-d).([0 \quad 1]X)$$

The averaging state space for resistive load will be:

$$X^{\cdot} = \begin{bmatrix} 0 & \frac{-1}{L} \\ \frac{1}{C} & \frac{-1}{RC} \end{bmatrix} X + \begin{bmatrix} \frac{2d-1}{L} \\ 0 \end{bmatrix} E \quad (15)$$

$$Y = [0 \quad 1]X$$

Then, the VSI-H bridge inverter is loaded with resistive - inductive load. This load change is modeled by deriving the operation states equations as follows:

For State (1): at the positive half cycle, T_1 and T_3 are ON, and by applying KVL, then:

$$-E + L\frac{di_L}{dt} + V_c = 0 \quad (16)$$

$$\frac{dV_c}{dt} = \frac{1}{C}(i_L - i_O) \quad (17)$$

$$V_c = R_f i_o + L_f \frac{di_o}{dt} \quad (18)$$

$$\frac{di_L}{dt} = \frac{1}{L}(E - V_c) \quad (19)$$

$$\frac{di_o}{dt} = \frac{1}{L_f}V_c - \frac{R_f}{L_f}i_o \quad (20)$$

$$V_o = V_c \quad (21)$$

The state space representation for state (1) will be:

$$X^{\cdot} = A_1 X + B_1 E$$
$$Y = C_1 X + D_1 E \quad (22)$$

Where

$$X = [i_L \quad V_c \quad i_o]^T$$

$$A_1 = \begin{bmatrix} 0 & \frac{-1}{L} & 0 \\ \frac{1}{C} & 0 & \frac{-1}{C} \\ 0 & \frac{1}{L_f} & \frac{-R_f}{L_f} \end{bmatrix} \qquad B_1 = \begin{bmatrix} \frac{1}{L} \\ 0 \\ 0 \end{bmatrix} \quad (23)$$

$$C_1 = [0 \quad 1 \quad 0] \qquad D_1 = [0]$$

For State (2), at the negative half cycle, T_2 and T_4 are ON, by applying KVL, then:

$$-E + L\frac{di_L}{dt} - V_c = 0 \quad (24)$$

$$\frac{dV_c}{dt} = \frac{1}{C}(i_L - i_O) \quad (25)$$

$$V_c = R_f i_o + L_f \frac{di_o}{dt} \quad (26)$$

$$\frac{di_L}{dt} = \frac{-1}{L}(E + V_c) \quad (27)$$

$$\frac{di_o}{dt} = \frac{1}{L_f}V_c - \frac{R_f}{L_f}i_o \quad (28)$$

$$V_o = V_c \quad (29)$$

The state space representation for state (2) will be:

$$X^{\cdot} = A_2 X + B_2 E$$
$$Y = C_2 X + D_2 E \quad (30)$$

Where

$$X = [i_L \quad V_c \quad i_o]^T$$

$$A_2 = \begin{bmatrix} 0 & \frac{-1}{L} & 0 \\ \frac{1}{C} & 0 & \frac{-1}{C} \\ 0 & \frac{1}{L_f} & \frac{-R_f}{L_f} \end{bmatrix} \qquad B_2 = \begin{bmatrix} \frac{-1}{L} \\ 0 \\ 0 \end{bmatrix}$$

$$C_2 = [0 \quad 1 \quad 0] \qquad D_2 = [0]$$

State space averaging technique is used to combine both two operation states in one state space representation as follows:

$$X^{\cdot} = d.(A_1X + B_1E) + (1-d).(A_2X + B_2E)$$

$$Y = d.(C_2X + D_2E) + (1-d).(C_2X + D_2E)$$

Averaging the state space for Ohmic - inductive load will be:

$$X^{\cdot} = \begin{bmatrix} 0 & \frac{-1}{L} & 0 \\ \frac{1}{C} & 0 & \frac{-1}{C} \\ 0 & \frac{1}{L_f} & \frac{-R_f}{L_f} \end{bmatrix} X + \begin{bmatrix} \frac{2d-1}{L} \\ 0 \\ 0 \end{bmatrix} E \quad (31)$$

$$Y = [0 \quad 1 \quad 0]X$$

2.3 Feedback Control Structure

When the inverter output reaches the load voltage, the output voltage on the load side is sensed by the voltage sensor and fed back to a subtractor which compares the load output to the reference signal (desired signal) and generates the voltage error signal. A proportional-integral (PI) controller receives this instantaneous error. The integral term in the PI controller enhances tracking by decreasing the instantaneous difference between the reference and the actual voltage. The error is forced to stay within the range specified by the triangular waveform's amplitude (modulation index). The controller signal will calculate the proper magnitude of the sine wave to be compared with a triangular carrier signal and the intersections will decide the switching frequency and pulse width, [20]. See Figure 3.

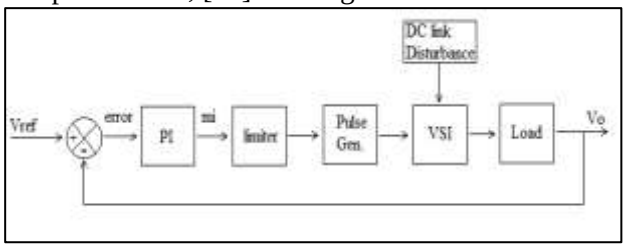

Fig. 3: Feedback control system of VSI-H bridge inverter.

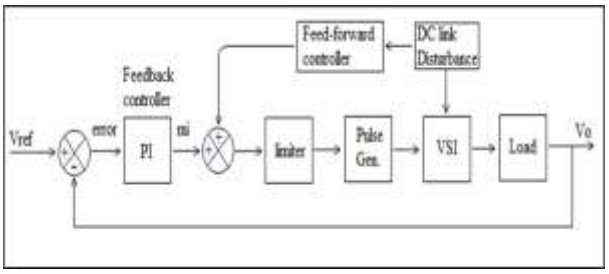

Fig. 4: Feedforward/Feedback control system of VSI.

2.4 Feed-forward/Feedback Control Structure

The feed forward control responds to change in command or measured disturbances in a pre-defined way. Based on the prediction ability of the plant behavior, it can react be-fore error takes place. On the other hand, the system response must be predictable to implement the feed forward structure. Moreover, it may not generalize to other conditions and will not be accurate if the system changes. Combining feed-forward with feedback control system is often used to provide the optimum response behavior of the plant due to merged advantages

of both control structures, [16]. In this paper, the combined control system is utilized to reject the DC input disturbance of VSI-H bridge and keep a stable voltage waveform at its terminal under load variations as shown in Figure 4.

3 The Proposed Feedforward / Feedback Control Implementation

There are many control systems for a single-phase voltage inverter to enable it to drive the required loads as efficiently as possible. However, due to the possibility of disturbances at more than one side of these systems, there is a need to merge two control systems. In the presented paper, the Feed-forward/Feedback (FF/FB) control system is pro-posed to control the generated output voltage and to reject the DC link voltage disturbance under various loads. This section illustrates the detailed model of VSI and the proposed control approach under disturbance - load variation.

3.1 Model Parameters

The feedback control structure is applied on the VSI-H bridge based on the parameter listed in Tables 2-7. Figure 6 illustrates the full details of the Simulink model. The inverter block is a H-bridge circuit with IGBT/diode as power switches. The controller tracks only the reference voltage

and is totally ignored to measure the DC link voltage disturbances. The model shows the Sinusoidal Pulse Width Modulation (SPWM) pulses generation and the low pass LC filter.

Then, the implementation of the combined control systems occurred using the parameter values in Tables 2 to 7. As shown in Figure 6, the static Feedforward control is used to reject the DC link disturbances and along with the feedback controller (PID), the output voltage is kept constant under load fluctuations. On the other hand, the total modulation index is determined by two values including the PID controller and the static gain which provides the better attenuation to the input disturbances.

Table 2. Inverter bridge design data

Parameter	Value
DC input (Volt)	200
Number of arms	2
Snubber resistance R_S (ohm)	$1e^7$
Snubber capacitance C_S (F)	Inf
Power electronics device	IGBT with diode
R_{ON} (ohm)	$1e^{-3}$

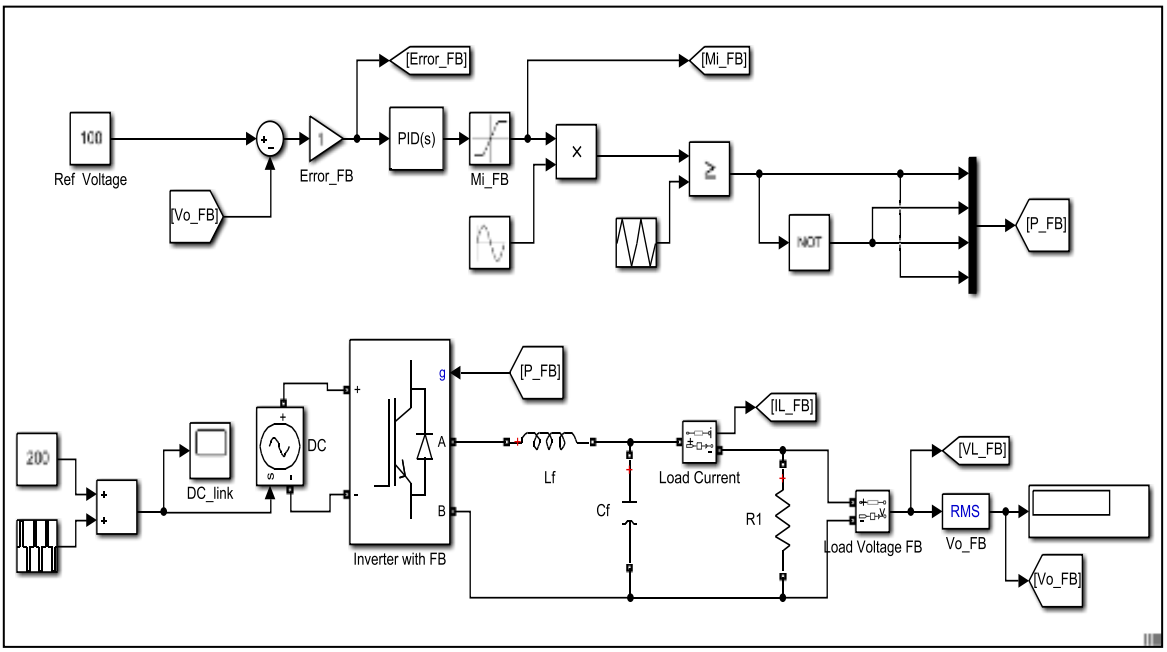

Fig. 5: Implemented feedback control with VSI-H bridge inverter.

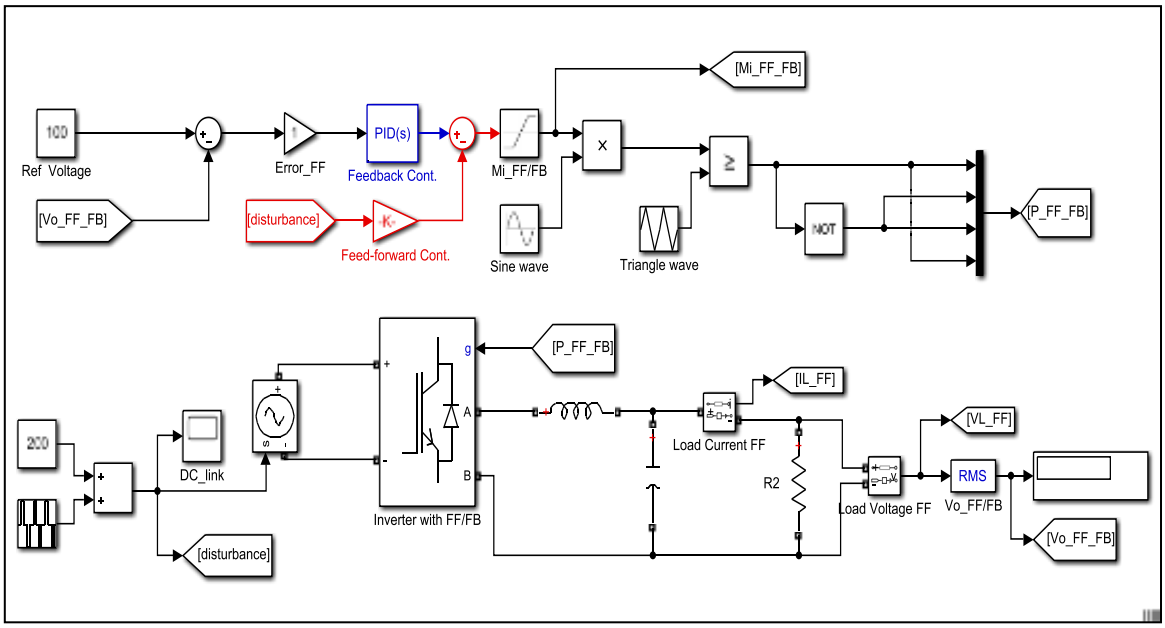

Fig. 6: Implemented FF/FB control with VSI-H bridge inverter.

Table 3. LC filter design data

Parameter	Value
Inductor (H)	$5e^{-3}$
Capacitor (F)	$50e^{-6}$

Table 4. SPWM pulse generation

Signal	Specifications
Fundamental wave	Sine wave 50 HZ

Table 5. Feedback system design data

Parameter	Value
Reference voltage (rms)	100 V
Proportional controller	$1e^{-5}$
Integral controller	0.28
Derivative controller	$1e^{-5}$
PID structure	Parallel
Output limitation	0.2 – 1

Table 6. Feedforward/Feedback controller data

Parameter	Value
Reference voltage (rms)	100 V
Proportional controller	$1e^{-5}$
Integral controller	0.28
Derivative controller	$1e^{-5}$
PID structure	Parallel
Output limitation	0.2 – 1
Static gain	0.001667
Carrier Wave	Zero phase shift Triangle wave 5000 HZ 90o phase shift

Table 7. Variable load data

Load	Specifications
Resistor	10 ohm.
Inductor	10e-3 H.
Single phase induction motor	Nominal voltage (rms) = 100 V.
	Capacitive Start.
	Nominal power = 186.5 VA.
	Frequency = 50 HZ.
	Torque = 1 p.u.

A full comparison will be made on both control systems (feedback and combined one) to investigate the inverter behavior. 15% of DC link disturbances as shown in Figure 7. For each case the load will be changed three times to engage the inverter with static load (Ohmic, Ohmic-inductive) or dynamic load such as induction motor.

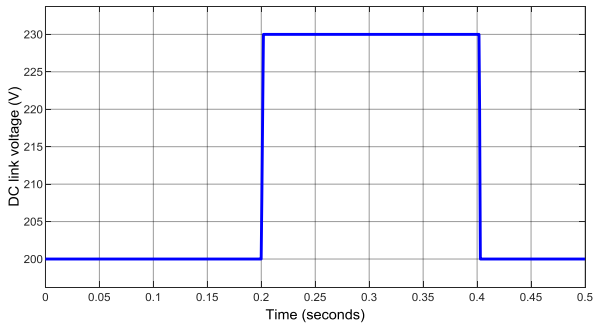

Fig. 7: DC link voltage with 15% disturbance

3.2 The Proposed Control Process

The combined control structure is used to reject the DC link fluctuations and to regulate the generated voltage of the VSI-H bridge inverter model in Figures 6 and 7. The proposed control strategy estimated the required modulation index to generate the proper SPWM pulses to the inverter bridge switching devices. The merged control criteria utilized the closed loop of classical PID controller, which uses a three mathematical operation to the produced error signal in order to apply accurate and optimal control of VSI-H bridge. Moreover, it applied the static feed-forward controller with the existing PID manipulator in order to improve the ability of the DC disturbance rejection. The control process can be explained as follows:

- The feedback controller (PID) will regulate the generated output voltage by measuring it and feeding it back to the error detector, which estimates the error between the reference and the produced voltages.
- The PID will produce a proper modulation index in order to generate the switching pulses.
- The static feed-forward controller will modify the modulation index value according to the DC link Disturbance.
- The modulation index value will be limited at the boundary of (0.2 - 1) using the saturation block, this step will ensure the linear behavior of the proposed controller.
- The modulation index value will specify the fundamental wave magnitude to be compared with the carrier signal and thus the generation of SPWM pulses.
- The generated pulses will be distributed on the four-switching device of the inverter bridge.
- The low pass LC circuit will filter the bridge output voltage before applying it to the load.
- Different load types were connected to the VSI output terminal to investigate its response.
- The same power system was controlled by only a feedback controller to com-pare its results with the proposed approach.

The proposed control method can be summarized by the flow chart, illustrated in Figure 8.

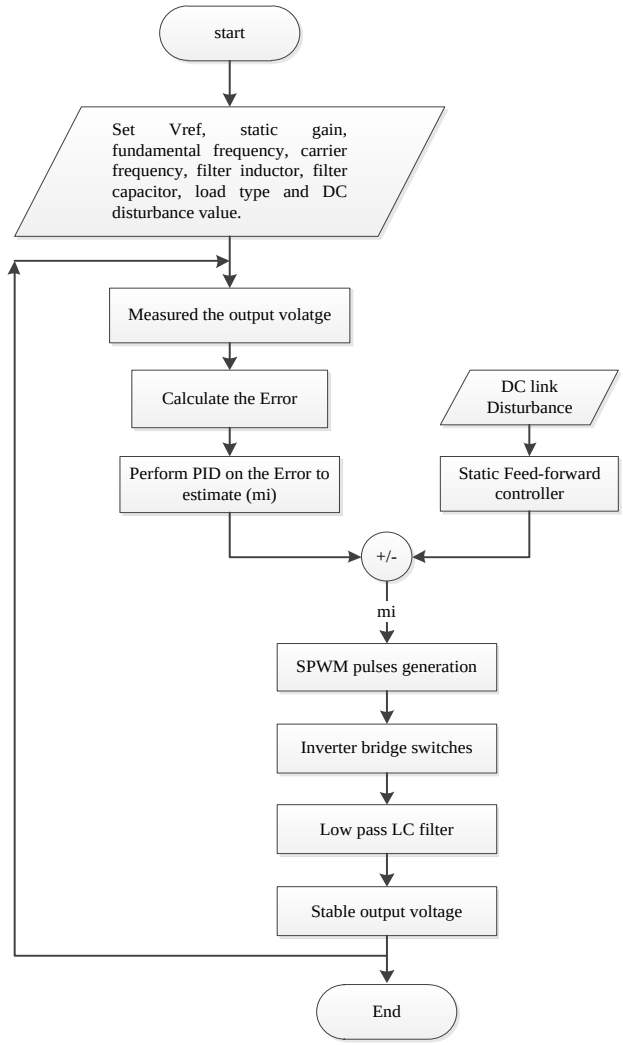

Fig. 8: Control process flow chart

4 Results and Discussion

Tables 8, 9, and 10 display the results for the system under different loads, R, RL, and induction motor. The results compare between using a feedback controller only and the proposed FFFB controller under disturbance. It can be seen that the merged control approach FFFB scores better performance than the feedback control in terms of overshoot, minimum settling, maximum settling, and peak values. However, it records close results to the feedback system in terms of rise and settling times. It can be shown that the proposed approach can handle disturbance rising and provide a more efficient response compared to the feedback system.

Table 8. Step responses of both control systems with ohmic load under 15% disturbances

Ohmic load results under 15% disturbance		
Parameter	Feed back	Feed forward + Feedback
Rise time (sec)	0.000361	0.000545
settling time (sec)	0.103576	0.103807
Settling Min (volt)	99.457572	99.749542
Settling Max (volt)	112.447286	105.619826
Over shoot	12.447286	5.619826
Peak (volt)	112.447286	105.619826
Peak time (sec)	0.021750	0.021712

Table 9. Step responses of both control systems with RL load under 15% disturbances

Resistive - inductive load results under 15% disturbance		
Parameter	Feed back	Feed forward + Feedback
Rise time (sec)	0.000376	0.000554
settling time (sec)	0.176280	0.103146
Settling Min (volt)	99.592600	99.817048
Settling Max (volt)	112.523055	105.925001
Over shoot	12.523055	5.925001
Peak (volt)	112.523055	105.925001
Peak time (sec)	0.021550	0.021550

Table 10. Step responses of both control systems with induction motor load under 15% disturbances

Induction motor results under 15% disturbance		
Parameter	Feed back	Feed forward + Feedback
Rise time (sec)	0.004629	0.001873
settling time (sec)	0.200000	0.200000
Settling Min (volt)	99.779150	99.955386
Settling Max (volt)	100.350549	100.314212
Over shoot	12.965064	6.546617
Peak (volt)	112.965064	106.546617
Peak time (sec)	0.020750	0.020750

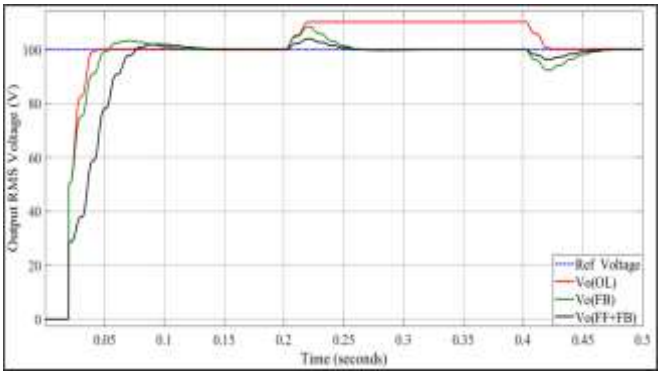

Fig. 9: Output RMS voltages of the conducted control systems under ohmic load

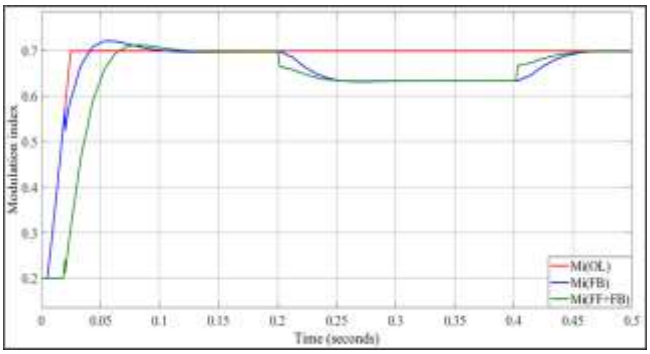

Fig. 10: Modulation indices responses of the conducted control systems under ohmic load

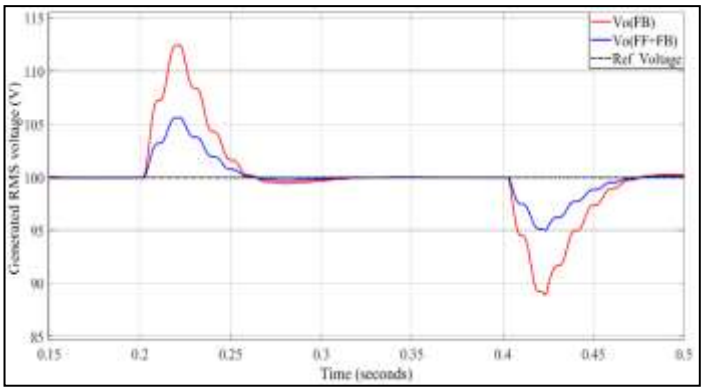

Fig. 11: Inverter RMS voltages of ohmic load under 15% disturbance.

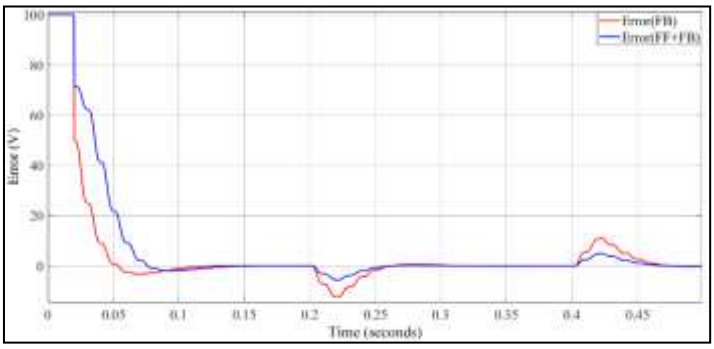

Fig. 12: Inverter RMS voltage errors of ohmic load under 15% disturbance.

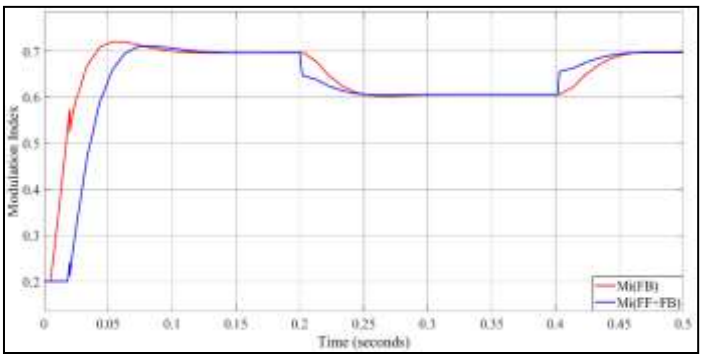

Fig. 13: Modulation index responses with ohmic load under 15% disturbance

The effectiveness of the proposed controller FFFB is shown for ohmic load only, the other loads RL, and the induction motor proves the same effective results. Figures 9 and 10 show the simulation results for RMS output voltages and the modulation index of VSI fed different loads using three different control types, the Open Loop (OL), the feedback (FB) and the proposed FFFB systems under disturbance of 15% of DC link value. It is notable that the open loop control is the fastest one with respect to rise and settling times, but it provides the worst response under disturbance. It can be seen that the remaining approaches

overcome the disturbance, but the merged system FFFB leads to more stable RMS voltages.

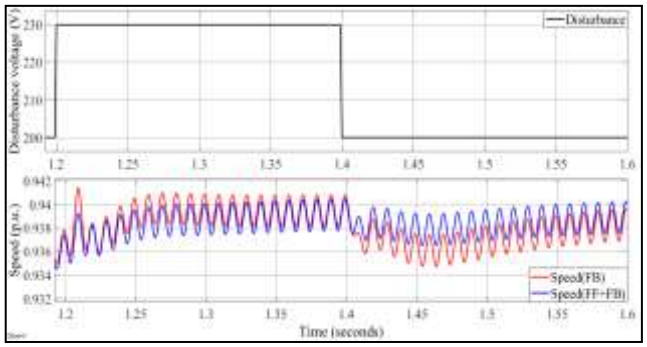

Fig. 14: Speed responses under full load with 15% disturbance.

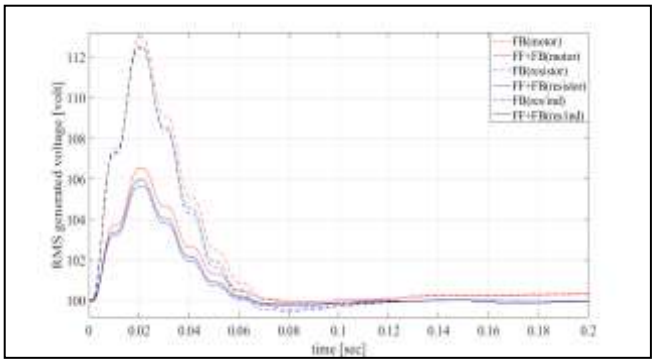

Fig. 15: RMS inverter voltages at 15% disturbance for different loads

Figures 11 to 13 show the simulation results for RMS output voltage, error, and the modulation index of closed loop control system using ohmic load only. It is notable that the proposed system FFFB provides minimum oscillation and overshoot and thus more stable voltage compared to the FB controller. The increment of disturbance can be handled as well with the superior proposed FFFB approach. For more convenience, a dynamic response for the proposed system is simulated. Figure 14 illustrates the speed response of dynamic rated load. It can be seen that applying more disturbance increases the motor speed.

Moreover, the superior performance of the proposed approach is proved in stabilizing the motor speed under rated load conditions. Figure 15 shows the performances of both control systems under variable loads as well as disturbance conditions. The proposed FFFB system shows the best performance in disturbance rejection regarding the load type and the fluctuation level. On the other hand, the overshoot values of voltage vary from one load type to another. It is notable that it is high in case of induction motor, and it is low in case of ohmic load.

5 Conclusion

In this paper, a new combined feedback/feed-forward FFFB controller for single-phase VSI is proposed under different loads and disturbance conditions. The mathematical and MATLAB models of the system are presented. The response and behaviour of the system under sudden change of DC link voltage of 15% are studied. Different scenarios are presented to prove the effectiveness of the proposed FFFB to enhance system stability and performance parameters such as overshoot, settling time, and rising time. The performance of the combined control system FFFB is assessed and compared with the other two control strategies, the open-loop, and the closed-loop feedback control systems. The proposed FFFB system enhances the behaviour and the performance parameters compared to other controllers. The proposed closed-loop controller (FFFB) can reduce the overshoot by 50% less than the feedback controller only. Also, the settling time has been improved by 41%, and 61% for RL and induction motors, respectively.

References:

[1] B. K. Bose, "Global energy scenario and impact of power electronics in 21st century," IEEE Transactions on Industrial Electronics, vol. 60, pp. 2638-2651, 2012.

[2] I. Colak, E. Kabalci, G. Fulli, and S. Lazarou, "A survey on the contributions of power electronics to smart grid systems," Renewable and Sustainable Energy Reviews, vol. 47, pp. 562-579, 2015.

[3] L. Hassaine, E. OLias, J. Quintero, and V. Salas, "Overview of power inverter topologies and control structures for grid con-nected photovoltaic systems," Renewable and Sustainable Energy Reviews, vol. 30, pp. 796-807, 2014.

[4] J. Jana, H. Saha, and K. D. Bhattacharya, "A review of inverter topologies for single-phase grid-connected photovoltaic systems," Renewable and Sustainable Energy Reviews, vol. 72, pp. 1256-1270, 2017.

[5] G. Ding et al., "Adaptive DC-Link Voltage Control of Two-Stage Photovoltaic Inverter During Low Voltage Ride-Through Operation," in IEEE Transactions on Power

Electronics, vol. 31, no. 6, pp. 4182-4194, June 2016, doi: 10.1109/TPEL.2015.2469603.

[6] T. Zhao, X. Zhang, W. Mao, F. Wang, J. Xu and Y. Gu, "A Modified Hybrid Modulation Strategy for Suppressing DC Voltage Fluctuation of Cascaded H-Bridge Photovoltaic Inverter," in IEEE Transactions on Industrial Electronics, vol. 65, no. 5, pp. 3932-3941, May 2018, doi: 10.1109/TIE.2017.2758758.

[7] K. A. Mahafzah, K. Krischan and A. Muetze, "Efficiency enhancement of a three phase Soft Switching Inverter under light load conditions," IECON 2016 - 42nd Annual Conference of the IEEE Industrial Electronics Society, 2016, pp. 3378-3383, doi: 10.1109/IECON.2016.7793310.

[8] K. Chen, S. L. Tian, and Y. H. Cheng, "Research on the Suppression of Input Power Disturbance for Single-Phase Photovoltaic Grid-Connected Inverter," in Applied Mechanics and Materials, 2012, pp. 243-246.

[9] S. Li and H. Xiong, "Active disturbance rejection control of single phase grid connected inverter," in 2016 IEEE International Conference on Mechatronics and Automation, 2016, pp. 2344-2348.

[10] E. Demirok, D. Sera, R. Teodorescu, P. Rodriguez, and U. Borup, "Clustered PV inverters in LV networks: An overview of impacts and comparison of voltage control strategies," in 2009 IEEE Electrical Power & Energy Conference (EPEC), 2009, pp. 1-6.

[11] M. Monfared and S. Golestan, "Control strategies for single-phase grid integration of small-scale renewable energy sources: A review," Renewable and Sustainable Energy Reviews, vol. 16, pp. 4982-4993, 2012.

[12] L. Calderone, L. Pinola, and V. Varoli, "Optimal feed-forward compensation for PWM DC/DC converters with'linear'and'quadratic'conversion ratio," IEEE transactions on power electronics, vol. 7, pp. 349-355, 1992.

[13] M. Ding, R. Yokoyama, and J. She, "Current control for the grid-connected single-phase photovoltaic inverter in microgrid based on an equivalent-input-disturbance approach," in ISGT 2014, 2014, pp. 1-5.

[14] Y. Bao, C. Wang, J. Jiang, C. Jiang, and C. Duan, "Adaptive feedforward compensation for voltage source disturbance rejection in DC–DC converters," IEEE Transactions on Control Systems Technology, vol. 26, pp. 344-351, 2017.

[15] S. Mohamed, A. Zayed, and O. Abolaeha, "New Feed-Forward/Feedback Generalized Minimum Variance Self-tuning Pole-placement Controller," in Proceeding of World Academy of Science, Engineering and Technology, 2009, pp. 998-1001.

[16] M. Yiming, P. Boyu, L. Gongqing, L. Yongwen, and Z. Deliang, "Feedforward Feedback Control Based on DQN," in 2020 Chinese Control And Decision Conference (CCDC), 2020, pp. 550-554.

[17] C. Wang, P. Yang, C. Ye, Y. Wang, and Z. Xu, "Voltage control strategy for three/single phase hybrid multimicrogrid," IEEE Transactions on Energy Conversion, vol. 31, pp. 1498-1509, 2016.

[18] D. Dong, F. Luo, D. Boroyevich, and P. Mattavelli, "Leakage current reduction in a single-phase bidirectional AC–DC full-bridge inverter," IEEE Transactions on Power Electronics, vol. 27, pp. 4281-4291, 2012.

[19] P. A. Dahono and A. Purwadi, "An LC filter design method for single-phase PWM inverters," in Proceedings of 1995 International Conference on Power Electronics and Drive Systems. PEDS 95, 1995, pp. 571-576.

[20] T. Qanbari and B. Tousi, "Single-Source Three-Phase Multilevel Inverter Assembled by Three-Phase Two-Level Inverter and Two Single-Phase Cascaded H-Bridge Inverters," in IEEE Transactions on Power Electronics, vol. 36, no. 5, pp. 5204-5212, May 2021, doi: 10.1109/TPEL.2020.3029870.

[21] I. A. Altawil, K. A. Mahafzah and A. A. Smadi, "Hybrid active power filter based on diode clamped inverter and hysteresis band current controller," 2012 2nd International Conference on Advances in Computational Tools for Engineering Applications (ACTEA), 2012, pp. 198-203, doi: 10.1109/ICTEA.2012.6462865.

[22] V. Jammala, S. Yellasiri, and A. K. Panda, "Development of a new hybrid multilevel inverter using modified carrier SPWM switching strategy," IEEE Transactions on Power Electronics, vol. 33, pp. 8192-8197, 2018.

[23] F. A. Khan and S. Nisar, "Design and analysis of feedback control system," in

2018 International Conference on Information and Communications Technology (ICOIACT), 2018, pp. 16-24.

[24] Mohammad A Obeidat, "Real-Time DC Servomotor Identification and Control of Mechanical Braking System for Vehicle-to-Vehicle Communication", International Journal of Computer Applications 182(40): 20-30, February 2019.

[25] Mohammad A Obeidat and Ali Hamad," Applying Two Controller Schemes to Improve Input Tracking and Noise Reduction in DC-DC converters", PRZEGLĄD ELEKTROTECHNICZNY, Jan 2019.

[26] Mohammad A Obeidat, L.Y. Wang, F. Lin, "Real-Time Parameter Estimation of PMDC Motors using Quantized Sensors", IEEE Transactions on Vehicular Technology, Vol. 62, Issue 6, pp. 1- 10, July 2013.

Contribution of Individual Authors to the Creation of a Scientific Article (Ghostwriting Policy)

"All authors contributed to the study conception and design. Material preparation, data collection by Mustafa Alzghoul, analysis of the results was performed by Mohammad Obeidat, Khaled Mahafzah, Mustafa Alzghoul, and Hesham Al Salem. The first draft of the manuscript was written by Mustafa Alzghoul, then it was reviewed by Mohammad Obeidat, Khaled Mahafzah and Hesham Al Salem. All authors commented on previous versions of the manuscript. All authors read and approved the final manuscript".